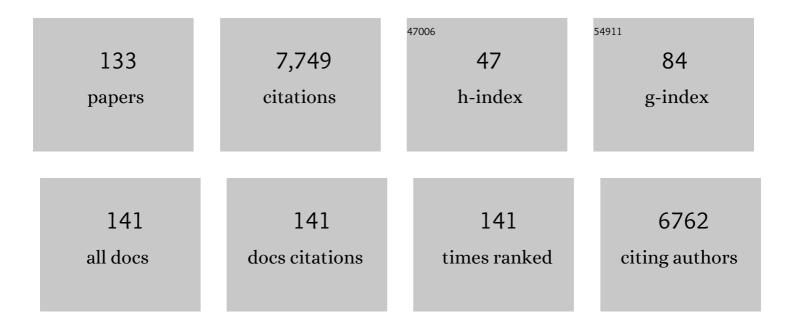
David Heslop

List of Publications by Year in descending order

Source: https://exaly.com/author-pdf/1554513/publications.pdf Version: 2024-02-01



#	Article	IF	CITATIONS
1	Directions Old and New: Palaeomagnetism and Fisher (1953) Meet Modern Statistics. International Statistical Review, 2022, 90, 237-258.	1.9	4
2	Organic carbon burial in Mediterranean sapropels intensified during Green Sahara Periods since 3.2 Myr ago. Communications Earth & Environment, 2022, 3, .	6.8	15
3	Unlocking information about fine magnetic particle assemblages from first-order reversal curve diagrams: Recent advances. Earth-Science Reviews, 2022, 227, 103950.	9.1	15
4	Assessment of Magnetic Techniques for Understanding Complex Mixtures of Magnetite and Hematite: The Inuyama Red Chert. Journal of Geophysical Research: Solid Earth, 2021, 126, .	3.4	5
5	Quantitative assessment of the oxygen isotope composition of fish otoliths from Lake Mungo, Australia. Quaternary Research, 2021, 102, 234-246.	1.7	1
6	Chronostratigraphy of a 270-ka sediment record from Lake Selina, Tasmania: Combining radiometric, geomagnetic and climatic dating. Quaternary Geochronology, 2021, 62, 101152.	1.4	4
7	Climatically Modulated Dust Inputs from New Zealand to the Southwest Pacific Sector of the Southern Ocean Over the Last 410 kyr. Paleoceanography and Paleoclimatology, 2021, 36, e2020PA003949.	2.9	2
8	Sea level and deep-sea temperature reconstructions suggest quasi-stable states and critical transitions over the past 40 million years. Science Advances, 2021, 7, .	10.3	29
9	A â^¼12 Myr Miocene Record of East Asian Monsoon Variability From the South China Sea. Paleoceanography and Paleoclimatology, 2021, 36, e2021PA004267.	2.9	26
10	Environmental magnetic fingerprinting of anthropogenic and natural atmospheric deposition over southwestern Europe. Atmospheric Environment, 2021, 261, 118568.	4.1	6
11	Lowâ€Temperature Magnetic Properties of Marine Sediments—Quantifying Magnetofossils, Superparamagnetism, and Maghemitization: Eastern Mediterranean Examples. Journal of Geophysical Research: Solid Earth, 2021, 126, e2021JB021793.	3.4	1
12	Magnetic Domain State and Anisotropy in Hematite (<i>α</i> â€Fe ₂ O ₃) From Firstâ€Order Reversal Curve Diagrams. Journal of Geophysical Research: Solid Earth, 2021, 126, e2021JB023027.	3.4	8
13	Mapping hydrocarbon charge-points in the Wessex Basin using seismic, geochemistry and mineral magnetics. Marine and Petroleum Geology, 2020, 111, 510-528.	3.3	12
14	Continental-scale magnetic properties of surficial Australian soils. Earth-Science Reviews, 2020, 203, 103028.	9.1	9
15	An Automatic Model Selectionâ€Based Machine Learning Framework to Estimate FORC Distributions. Journal of Geophysical Research: Solid Earth, 2020, 125, e2020JB020418.	3.4	9
16	Assessment and Integration of Bulk and Componentâ€ S pecific Methods for Identifying Mineral Magnetic Assemblages in Environmental Magnetism. Journal of Geophysical Research: Solid Earth, 2020, 125, e2019JB019024.	3.4	7
17	Micromagnetic simulations of first-order reversal curve (FORC) diagrams of framboidal greigite. Geophysical Journal International, 2020, 222, 1126-1134.	2.4	14
18	Coupling of Indo-Pacific climate variability over the last millennium. Nature, 2020, 579, 385-392.	27.8	116

#	Article	IF	CITATIONS
19	Uncertainty Propagation in Hierarchical Paleomagnetic Reconstructions. Journal of Geophysical Research: Solid Earth, 2020, 125, e2020JB019488.	3.4	11
20	Detrital remanent magnetization of single-crystal silicates with magnetic inclusions: constraints from deposition experiments. Geophysical Journal International, 2020, 224, 2001-2015.	2.4	11
21	Hematite (α-Fe2O3) quantification in sedimentary magnetism: limitations of existing proxies and ways forward. Geoscience Letters, 2020, 7, .	3.3	30
22	Dredging and canal gate technologies in Portus, the ancient harbour of Rome, reconstructed from event stratigraphy and multi-proxy sediment analysis. Quaternary International, 2019, 511, 78-93.	1.5	5
23	Paleomagnetic Recording Efficiency of Sedimentary Magnetic Mineral Inclusions: Implications for Relative Paleointensity Determinations. Journal of Geophysical Research: Solid Earth, 2019, 124, 6267-6279.	3.4	7
24	Dating of tsunami boulders from Ishigaki Island, Japan, with a modified viscous remanent magnetization approach. Earth and Planetary Science Letters, 2019, 520, 94-104.	4.4	4
25	Domain State Diagnosis in Rock Magnetism: Evaluation of Potential Alternatives to the Day Diagram. Journal of Geophysical Research: Solid Earth, 2019, 124, 5286-5314.	3.4	44
26	Simulation of Remanent, Transient, and Induced FORC Diagrams for Interacting Particles With Uniaxial, Cubic, and Hexagonal Anisotropy. Journal of Geophysical Research: Solid Earth, 2019, 124, 12404-12429.	3.4	18
27	Quantifying the Similarity of Paleomagnetic Poles. Journal of Geophysical Research: Solid Earth, 2019, 124, 12388-12403.	3.4	11
28	Midlatitude Southern Hemisphere Temperature Change at the End of the Eocene Greenhouse Shortly Before Dawn of the Oligocene Icehouse. Paleoceanography and Paleoclimatology, 2019, 34, 1995-2004.	2.9	4
29	An Improved Algorithm for Unmixing Firstâ€Order Reversal Curve Diagrams Using Principal Component Analysis. Geochemistry, Geophysics, Geosystems, 2018, 19, 1595-1610.	2.5	56
30	A Critical Appraisal of the "Day―Diagram. Journal of Geophysical Research: Solid Earth, 2018, 123, 2618-2644.	3.4	153
31	Magnetic Domain State Diagnosis in Soils, Loess, and Marine Sediments From Multiple Firstâ€Order Reversal Curveâ€Type Diagrams. Journal of Geophysical Research: Solid Earth, 2018, 123, 998-1017.	3.4	9
32	A Bayesian Approach to the Paleomagnetic Conglomerate Test. Journal of Geophysical Research: Solid Earth, 2018, 123, 1132-1142.	3.4	7
33	Tropical Indo-Pacific hydroclimate response to North Atlantic forcing during the last deglaciation as recorded by a speleothem from Sumatra, Indonesia. Earth and Planetary Science Letters, 2018, 492, 264-278.	4.4	44
34	Coupled microbial bloom and oxygenation decline recorded by magnetofossils during the Palaeocene–Eocene Thermal Maximum. Nature Communications, 2018, 9, 4007.	12.8	56
35	Magnetic vortex effects on first-order reversal curve (FORC) diagrams for greigite dispersions. Earth and Planetary Science Letters, 2018, 501, 103-111.	4.4	21
36	Signatures of Reductive Magnetic Mineral Diagenesis From Unmixing of Firstâ€Order Reversal Curves. Journal of Geophysical Research: Solid Earth, 2018, 123, 4500-4522.	3.4	61

#	Article	IF	CITATIONS
37	Revisiting the Paleomagnetic Reversal Test: A Bayesian Hypothesis Testing Framework for a Common Mean Direction. Journal of Geophysical Research: Solid Earth, 2018, 123, 7225-7236.	3.4	20
38	Measuring, Processing, and Analyzing Hysteresis Data. Geochemistry, Geophysics, Geosystems, 2018, 19, 1925-1945.	2.5	64
39	Influence of Sea Level Change and Centennial East Asian Monsoon Variations on Northern South China Sea Sediments Over the Past 36 kyr. Geochemistry, Geophysics, Geosystems, 2018, 19, 1674-1689.	2.5	13
40	Southernmost evidence of large European Ice Sheet-derived freshwater discharges during the Heinrich Stadials of the Last Glacial Period (Galician Interior Basin, Northwest Iberian Continental) Tj ETQq0 0 0	rgB 4.4 0ver	loc 2 210 Tf 50
41	Magnetic domain state diagnosis using hysteresis reversal curves. Journal of Geophysical Research: Solid Earth, 2017, 122, 4767-4789.	3.4	65
42	Volcanic records of the Laschamp geomagnetic excursion from Mt Ruapehu, New Zealand. Earth and Planetary Science Letters, 2017, 472, 131-141.	4.4	17
43	Remanence acquisition efficiency in biogenic and detrital magnetite and recording of geomagnetic paleointensity. Geochemistry, Geophysics, Geosystems, 2017, 18, 1435-1450.	2.5	37
44	A 3 million year index for North African humidity/aridity and the implication of potential pan-African Humid periods. Quaternary Science Reviews, 2017, 171, 100-118.	3.0	108
45	Penultimate deglacial warming across the Mediterranean Sea revealed by clumped isotopes in foraminifera. Scientific Reports, 2017, 7, 16572.	3.3	42
46	Resolving the Origin of Pseudo‣ingle Domain Magnetic Behavior. Journal of Geophysical Research: Solid Earth, 2017, 122, 9534-9558.	3.4	145
47	A 17,000 yr paleomagnetic secular variation record from the southeast Alaskan margin: Regional and global correlations. Earth and Planetary Science Letters, 2017, 473, 177-189.	4.4	20
48	Dominant 100,000-year precipitation cyclicity in a late Miocene lake from northeast Tibet. Science Advances, 2017, 3, e1600762.	10.3	114
49	Estimation and propagation of uncertainties associated with paleomagnetic directions. Journal of Geophysical Research: Solid Earth, 2016, 121, 2274-2289.	3.4	14
50	Unmixing hysteresis loops of the late Miocene–early Pleistocene loess-red clay sequence. Scientific Reports, 2016, 6, 29515.	3.3	6
51	Widespread occurrence of silicateâ€hosted magnetic mineral inclusions in marine sediments and their contribution to paleomagnetic recording. Journal of Geophysical Research: Solid Earth, 2016, 121, 8415-8431.	3.4	65
52	The pseudo-Thellier palaeointensity method: new calibration and uncertainty estimates. Geophysical Journal International, 2016, 207, 1596-1608.	2.4	30
53	Estimating the concentration of aluminumâ€substituted hematite and goethite using diffuse reflectance spectrometry and rock magnetism: Feasibility and limitations. Journal of Geophysical Research: Solid Earth, 2016, 121, 4180-4194.	3.4	28
54	Magnetism of Alâ€substituted magnetite reduced from Alâ€hematite. Journal of Geophysical Research: Solid Earth, 2016, 121, 4195-4210.	3.4	18

#	Article	IF	CITATIONS
55	Analyzing paleomagnetic data: To anchor or not to anchor?. Journal of Geophysical Research: Solid Earth, 2016, 121, 7742-7753.	3.4	29
56	Asian monsoon modulation of nonsteady state diagenesis in hemipelagic marine sediments offshore of <scp>J</scp> apan. Geochemistry, Geophysics, Geosystems, 2016, 17, 4383-4398.	2.5	22
57	Discrimination of biogenic and detrital magnetite through a double Verwey transition temperature. Journal of Geophysical Research: Solid Earth, 2016, 121, 3-14.	3.4	69
58	New methods for unmixing sediment grain size data. Geochemistry, Geophysics, Geosystems, 2015, 16, 4494-4506.	2.5	241
59	A protocol for variableâ€resolution firstâ€order reversal curve measurements. Geochemistry, Geophysics, Geosystems, 2015, 16, 1364-1377.	2.5	61
60	Testing the use of viscous remanent magnetisation to date flood events. Frontiers in Earth Science, 2015, 3, .	1.8	5
61	Bipolar seesaw control on last interglacial sea level. Nature, 2015, 522, 197-201.	27.8	131
62	Source-to-sink magnetic properties of NE Saharan dust in Eastern Mediterranean marine sediments: review and paleoenvironmental implications. Frontiers in Earth Science, 2015, 3, .	1.8	12
63	Numerical strategies for magnetic mineral unmixing. Earth-Science Reviews, 2015, 150, 256-284.	9.1	62
64	Prediction of Geochemical Composition from XRF Core Scanner Data: A New Multivariate Approach Including Automatic Selection of Calibration Samples and Quantification of Uncertainties. Developments in Paleoenvironmental Research, 2015, , 507-534.	8.0	96
65	Soil moisture balance and magnetic enhancement in loess–paleosol sequences from the Tibetan Plateau and Chinese Loess Plateau. Earth and Planetary Science Letters, 2015, 409, 120-132.	4.4	56
66	Terrigenous input off northern South America driven by changes in Amazonian climate and the North Brazil Current retroflection during the last 250 ka. Climate of the Past, 2014, 10, 843-862.	3.4	66
67	Syntectonic emplacement of Late Cretaceous mafic dyke swarms in coastal southeastern China: Insights from magnetic fabrics, rock magnetism and field evidence. Tectonophysics, 2014, 637, 328-340.	2.2	12
68	A statistical simulation of magnetic particle alignment in sediments. Geophysical Journal International, 2014, 197, 828-837.	2.4	12
69	A Holocene record of coastal landscape dynamics in the eastern Kimberley region, Australia. Journal of Quaternary Science, 2014, 29, 163-174.	2.1	23
70	Understanding fine magnetic particle systems through use of first-order reversal curve diagrams. Reviews of Geophysics, 2014, 52, 557-602.	23.0	310
71	Magnetic detection and characterization of biogenic magnetic minerals: A comparison of ferromagnetic resonance and firstâ€order reversal curve diagrams. Journal of Geophysical Research: Solid Earth, 2014, 119, 6136-6158.	3.4	42
72	Late Miocene-early Pleistocene paleoclimate history of the Chinese Loess Plateau revealed by remanence unmixing. Geophysical Research Letters, 2014, 41, 2163-2168.	4.0	33

#	Article	IF	CITATIONS
73	Variable remanence acquisition efficiency in sediments containing biogenic and detrital magnetites: Implications for relative paleointensity signal recording. Geochemistry, Geophysics, Geosystems, 2014, 15, 2780-2796.	2.5	34
74	Is there a link between geomagnetic reversal frequency and paleointensity? A Bayesian approach. Journal of Geophysical Research: Solid Earth, 2014, 119, 5290-5304.	3.4	21
75	Sea-level variability over five glacial cycles. Nature Communications, 2014, 5, 5076.	12.8	325
76	Insights into magmatic processes and hydrothermal alteration of in situ superfast spreading ocean crust at ODP/IODP site 1256 from a cluster analysis of rock magnetic properties. Geochemistry, Geophysics, Geosystems, 2014, 15, 3430-3447.	2.5	13
77	Characterizing magnetofossils from firstâ€order reversal curve (FORC) central ridge signatures. Geochemistry, Geophysics, Geosystems, 2014, 15, 2170-2179.	2.5	51
78	Magnetic paleointensity stratigraphy and high-resolution Quaternary geochronology: successes and future challenges. Quaternary Science Reviews, 2013, 61, 1-16.	3.0	110
79	Magnetic properties of pelagic marine carbonates. Earth-Science Reviews, 2013, 127, 111-139.	9.1	84
80	Calculating uncertainties on predictions of palaeoprecipitation from the magnetic properties of soils. Global and Planetary Change, 2013, 110, 379-385.	3.5	18
81	Climatic control of magnetic granulometry in the Mircea Vod A_f loess/paleosol sequence (Dobrogea,) Tj ETQq1	1 0. <u>78</u> 431	4 rggT /Overl
82	Quantifying magnetite magnetofossil contributions to sedimentary magnetizations. Earth and Planetary Science Letters, 2013, 382, 58-65.	4.4	44
83	Lowâ€ŧemperature magnetic properties of pelagic carbonates: Oxidation of biogenic magnetite and identification of magnetosome chains. Journal of Geophysical Research: Solid Earth, 2013, 118, 6049-6065.	3.4	50
84	Abrupt shifts of the Sahara–Sahel boundary during Heinrich stadials. Climate of the Past, 2013, 9, 1181-1191.	3.4	71
85	Boundary scavenging at the East Atlantic margin does not negate use of 231Pa/230Th to trace Atlantic overturning. Earth and Planetary Science Letters, 2012, 333-334, 317-331.	4.4	29
86	Distribution of major elements in Atlantic surface sediments (36°N–49°S): Imprint of terrigenous input and continental weathering. Geochemistry, Geophysics, Geosystems, 2012, 13, .	2.5	170
87	Estimating best fit binary mixing lines in the Day plot. Journal of Geophysical Research, 2012, 117, .	3.3	14
88	A method for unmixing magnetic hysteresis loops. Journal of Geophysical Research, 2012, 117, .	3.3	38
89	Estimation of significance levels and confidence intervals for firstâ€order reversal curve distributions. Geochemistry, Geophysics, Geosystems, 2012, 13, .	2.5	57
90	Multiproxy characterization and budgeting of terrigenous endâ€members at the NW African continental margin. Geochemistry, Geophysics, Geosystems, 2012, 13, .	2.5	20

#	Article	IF	CITATIONS
91	Searching for single domain magnetite in the "pseudoâ€singleâ€domain―sedimentary haystack: Implications of biogenic magnetite preservation for sediment magnetism and relative paleointensity determinations. Journal of Geophysical Research, 2012, 117, .	3.3	143
92	Fingerprinting of the Atlantic meridional overturning circulation in climate models to aid in the design of proxy investigations. Climate Dynamics, 2012, 38, 1047-1064.	3.8	6
93	A Preisach method for estimating absolute paleofield intensity under the constraint of using only isothermal measurements: 1. Theoretical framework. Journal of Geophysical Research, 2011, 116, .	3.3	22
94	A Preisach method for estimating absolute paleofield intensity under the constraint of using only isothermal measurements: 2. Experimental testing. Journal of Geophysical Research, 2011, 116, .	3.3	20
95	Magnetotactic bacterial abundance in pelagic marine environments is limited by organic carbon flux and availability of dissolved iron. Earth and Planetary Science Letters, 2011, 310, 441-452.	4.4	150
96	Post-depositional remanent magnetization lock-in for marine sediments deduced from 10Be and paleomagnetic records through the Matuyama–Brunhes boundary. Earth and Planetary Science Letters, 2011, 311, 39-52.	4.4	73
97	Can oceanic paleothermometers reconstruct the Atlantic Multidecadal Oscillation?. Climate of the Past, 2011, 7, 151-159.	3.4	6
98	Interhemispheric symmetry of the tropical African rainbelt over the past 23,000 years. Nature Geoscience, 2011, 4, 42-45.	12.9	110
99	Diagnosing the uncertainty of taxa relative abundances derived from count data. Marine Micropaleontology, 2011, 79, 114-120.	1.2	12
100	The Senegal River mud belt: A high-resolution archive of paleoclimatic change and coastal evolution. Marine Geology, 2010, 278, 150-164.	2.1	37
101	Concurrent tectonic and climatic changes recorded in upper Tortonian sediments from the Eastern Mediterranean. Terra Nova, 2010, 22, 52-63.	2.1	5
102	Deriving confidence in paleointensity estimates. Geochemistry, Geophysics, Geosystems, 2010, 11, .	2.5	28
103	Reduced North Atlantic Central Water formation in response to early Holocene iceâ€sheet melting. Geophysical Research Letters, 2010, 37, .	4.0	18
104	Anthropogenic Forcings on the Surficial Osmium Cycle. Environmental Science & Technology, 2010, 44, 881-887.	10.0	23
105	Late Miocene paleoenvironmental changes in North Africa and the Mediterranean recorded by geochemical proxies (Monte Cibliscemi section, Sicily). Palaeogeography, Palaeoclimatology, Palaeoeclimatology, Palaeoecology, 2010, 285, 66-73.	2.3	16
106	Increase in African dust flux at the onset of commercial agriculture in the Sahel region. Nature, 2010, 466, 226-228.	27.8	247
107	On the statistical analysis of the rock magnetic S-ratio. Geophysical Journal International, 2009, 178, 159-161.	2.4	45
108	End-member modelling of isothermal remanent magnetization (IRM) acquisition curves: a novel approach to diagnose remagnetization. Geophysical Journal International, 2009, 178, 693-701.	2.4	28

#	Article	IF	CITATIONS
109	Thermal fluctuation fields in basalts. Earth, Planets and Space, 2009, 61, 111-117.	2.5	5
110	Salt production in pre-Funan Vietnam: archaeomagnetic reorientation of briquetage fragments. Journal of Archaeological Science, 2009, 36, 84-89.	2.4	4
111	Millennialâ€scale northwest African droughts related to Heinrich events and Dansgaardâ€Oeschger cycles: Evidence in marine sediments from offshore Senegal. Paleoceanography, 2009, 24, .	3.0	84
112	Correlation of Himalayan exhumation rates and Asian monsoon intensity. Nature Geoscience, 2008, 1, 875-880.	12.9	604
113	Tracking provenance change during the late Miocene in the eastern Mediterranean using geochemical and environmental magnetic parameters. Geochemistry, Geophysics, Geosystems, 2008, 9, .	2.5	19
114	Rock magnetic identification and geochemical process models of greigite formation in Quaternary marine sediments from the Gulf of Mexico (IODP Hole U1319A). Earth and Planetary Science Letters, 2008, 275, 233-245.	4.4	100
115	A wavelet investigation of possible orbital influences on past geomagnetic field intensity. Geochemistry, Geophysics, Geosystems, 2007, 8, n/a-n/a.	2.5	10
116	Unmixing magnetic remanence curves withouta prioriknowledge. Geophysical Journal International, 2007, 170, 556-566.	2.4	92
117	Using non-negative matrix factorization in the "unmixing―of diffuse reflectance spectra. Marine Geology, 2007, 241, 63-78.	2.1	45
118	The role of magnetostatic interactions in sediment suspensions. Geophysical Journal International, 2006, 165, 775-785.	2.4	14
119	Aspects of calculating first-order reversal curve distributions. Journal of Magnetism and Magnetic Materials, 2005, 288, 155-167.	2.3	48
120	A Monte Carlo investigation of the representation of thermally activated single-domain particles within the Day plot. Studia Geophysica Et Geodaetica, 2005, 49, 163-176.	0.5	8
121	Assessing the ability of first-order reversal curve (FORC) diagrams to unravel complex magnetic signals. Journal of Geophysical Research, 2005, 110, .	3.3	63
122	Using time- and temperature-dependent Preisach models to investigate the limitations of modelling isothermal remanent magnetization acquisition curves with cumulative log Gaussian functions. Geophysical Journal International, 2004, 157, 55-63.	2.4	123
123	Influence of magnetostatic interactions on first-order-reversal-curve (FORC) diagrams: a micromagnetic approach. Geophysical Journal International, 2004, 158, 888-897.	2.4	106
124	Title is missing!. Studia Geophysica Et Geodaetica, 2003, 47, 255-274.	0.5	19
125	Timing and structure of the mid-Pleistocene transition: records from the loess deposits of northern China. Palaeogeography, Palaeoclimatology, Palaeoecology, 2002, 185, 133-143.	2.3	62
126	Spectral analysis of unevenly spaced climatic time series using CLEAN: signal recovery and derivation of significance levels using a Monte Carlo simulation. Physics of the Earth and Planetary Interiors, 2002, 130, 103-116.	1.9	53

#	Article	IF	CITATIONS
127	Analysis of isothermal remanent magnetization acquisition curves using the expectation-maximization algorithm. Geophysical Journal International, 2002, 148, 58-64.	2.4	243
128	Quantification of magnetic coercivity components by the analysis of acquisition curves of isothermal remanent magnetisation. Earth and Planetary Science Letters, 2001, 189, 269-276.	4.4	622
129	A new astronomical timescale for the loess deposits of Northern China. Earth and Planetary Science Letters, 2000, 184, 125-139.	4.4	191
130	The new hominid skeleton from Sterkfontein, South Africa: age and preliminary assessment. Journal of Quaternary Science, 1999, 14, 293-298.	2.1	67
131	Sub-millennial scale variations in East Asian monsoon systems recorded by dust deposits from the north-western Chinese Loess Plateau. Physics and Chemistry of the Earth, 1999, 24, 785-792.	0.6	34
132	Are hydrodynamic shape effects important when modelling the formation of depositional remanent magnetization?. Geophysical Journal International, 0, 171, 1029-1035.	2.4	23
133	Data report: natural remanent magnetization of IODP Holes U1319A, U1320A, U1322B, and U1324B and magnetic carrier identification by scanning electron microscopy. Proceedings of the Integrated Ocean Drilling Program Integrated Ocean Drilling Program, 0, , .	1.0	1